Information Release Forms For

Global Scale Observations Of Ionospheric Instabilities From GPS In Low Earth Orbit

Leonard Kramer and John L. Goodman

The attached paper concerns the detection of ionospheric scintillation in velocity data from the Miniaturized Airborne Global Positioning System (GPS) Receiver (MAGR). Much of the paper concerns the geophysical aspects of scintillation.

It was originally approved for public release and presentation at the AIAA "Space 2001 ... The Odyssey Continues" Conference & Exposition, in Albuquerque NM, August 28-30, 2001. It has been updated, and we propose to submit it for consideration by the editors of the AIAA Journal of Spacecraft and Rockets.

New material is highlighted.

GLOBAL SCALE OBSERVATIONS OF IONOSPHERIC INSTABILITIES FROM GPS IN LOW EARTH ORBIT

Leonard Kramer* and John L. Goodman*
Navigation, United Space Alliance L.L.C., Houston

ABSTRACT

The GPS receiver used for navigation on the Space Shuttle exhibits range rate noise which appears to result from scintillation of the satellite signals by irregularities in ionospheric plasma. The noise events cluster in geographic regions previously identified as susceptible to instability and disturbed ionospheric conditions. These mechanisms are reviewed in the context of the GPS observations. Range rate data continuously monitored during the free orbiting phase of several space shuttle missions reveals global scale distribution of ionospheric irregularities. Equatorial events cluster +/- 20 degrees about the magnetic equator and polar events exhibit hemispheric asymmetry suggesting influence of off axis geomagnetic polar oval system. The diurnal, seasonal and geographic distribution is compared to previous work concerning equatorial spread F, Appleton anomaly and polar oval. The observations provide a succinct demonstration of the utility of space based ionospheric monitoring using GPS. The susceptability of GPS receivers to scintillation represents an unanticipated technical risk not factored into the selection of receivers for the United States space program.

* Navigation, United Space Alliance, L.L.C.
600 Gemini Avenue, USH-485L, Houston, Texas 77058 USA

NOMENCLATURE

Symbols:

c, the speed of light (a constant.)

E, Electric field of an electro-magnetic radiation.

V, spacecraft velocity.

S_n, an arbitrary path in space between transmitter and receiver.

α, angle from spacecraft velocity vector to line of sight to GPS satellite.

β, angle between spacecraft velocity vector and local geomagnetic field.

ε, permittivity of material media (e.g. ionospheric plasma.)

ε_0, permittivity of free space, a physical constant.

ϕ, phase of electro-magnetic radiation resulting from propagation in space.

Φ, phase envelope of an interference distribution.

ω, circular frequency of radiation (radians per unit time.)

ω_P, plasma frequency of radiation (radians per unit time.)

Other notation:

$\vec{A}$, a 3 component space vector.

$A_\perp$, perpendicular component of a vector.

$A_\parallel$, parallel component of a vector.

INTRODUCTION

In evaluating the implementation of the MAGR/S GPS receiver for eventual replacement of on-board TACAN systems currently in use for the United States shuttle program we have incidentally observed rather un-ambiguous evidence of ionospheric scintillation in the receiver velocity measurements.[1] The MAGR/S is a five channel, dual frequency, keyed receiver specially adapted by the manufacturer, Rockwell-Collins, for space flight use.[2] In the early phases of receiver evaluation, periods of noisy velocity in the output state from the GPS receiver were observed by ground controllers. The phenomenon, seen in Figure 1, was seen on many consecutive orbits and would persist for 10 to up to 20 minutes. Subsequent analysis indicates that this noise is related to delta phase, range rate measurements which usually cluster around the magnetic equator. The noise is a source of concern to the manned space effort as it exceeds nominal system requirement thresholds.

Since at least the early 1950's, ionospheric irregularities have been known to contribute to interruptions in radio communication. This disturbance is known as scintillation and the processes creating it show global scale effects. Many studies document observational and theoretical basis for scintillation of radio frequency radiation. Most important of these involve instability processes connected with neutral thermospheric atmosphere circulation and the geomagnetic field in equatorial regions and particle precipitation related to aurora in the polar cap latitudes. Aarons[3] has articulated theories related to

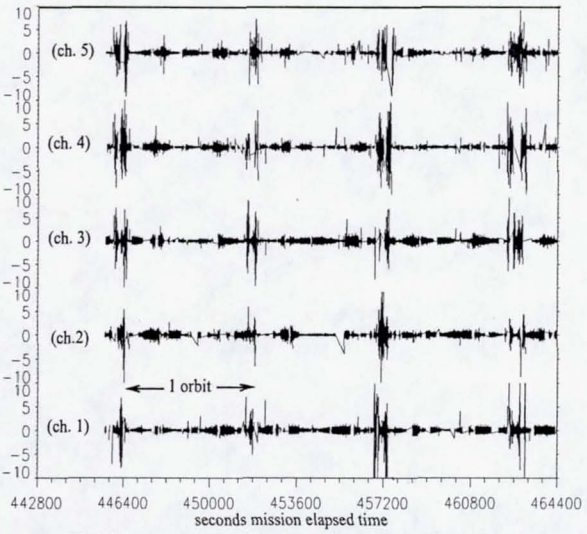

Figure 1. Evidence of scintillation of MAGR/S on STS 99 orbits. The range rate residuals are normalized to the projection of receiver state error in the range rate space.

the geographic and seasonal occurrence of equatorial scintillation. The book by Kelley has extensive discussion on the geophysical causes and consequences of ionospheric irregularities.[4] Efforts have been undertaken to create GPS based ionosphere monitoring systems based on ground based systems.[5,6]

The GPS system, utilizing a dual L band frequency (1.57542 and 1.2276 GHz) signal, is subject to scintillation and can be used to monitor the global nature of ionospheric processes contributing to scintillation and perhaps better understand these processes. We assert that the noise seen in the velocity are a result of ionospheric scintillation of the range rate measurements. In this work we develop techniques to diagnose scintillation from range rate measurements. We present geographic and to the extent possible, the seasonal and solar hour angle dependence of our events. We also describe a theoretical basis for spacecraft velocity augmentation of the effect and observational evidence supporting it.

We would like to advance the idea that satellite borne GPS receivers in low earth orbit can contribute to global understanding of occurrence and geophysical causes of ionospheric irregularities. Also, scintillation of GPS is one of the several factors that contribute to the technical risk of using off the shelf terrestrial based receivers for high performance applications.

DATA

As part of GPS receiver evaluation, auxiliary instrumentation port data is regularly collected during orbital phases of shuttle flights. These data comprise internal software parameters, pseudo-range and delta-phase range rate information in 4 simultaneously tracked GPS satellites and an additional peripheral channel that monitors satellite selection and the dual frequency correction needed to compensate for ionospheric delay.

The MAGR/S receiver software computes a state (position and velocity) using a blended solu-

tion "Kalman" filter employing process noise intentionally tuned to sub-optimum levels. The practice makes the receiver generically robust since uncertainty in the filter state grows quickly when measurements are absent and thus current measurements are always heavily weighted in the solution. It is fair to say that, in a sense, the receiver is not using a Kalman filter, rather that it delivers a blended deterministic solution. The downside to the practice is that the receiver is not optimal for space based application and has higher state uncertainty than is otherwise possible based on available gravity and drag models. For these reasons the receiver does not propagate its state well when measurements are absent.

Range Rate Measurements

The data in this investigation comprise 0.2 second period, phase change observables constituting range-rate measurements. Both pseudo-range and range rate are incorporated into the receiver's state estimate. Inertial information is contributed in the form of aiding data from the shuttle on-board solution and a barometric reading is used to augment altitude on entry and landing. As part of the usual state processing in the GPS internal filter, residuals are formed representing a difference between the state's projection of range rate and the actual range rate measurement. These residuals are then normalized to the projection of the Kalman filter covariance in the range rate space. Figure 1 presents a time series of some of these observations from a shuttle mission in February of 2000. These signatures form the principle evidence of scintillation that we have seen.

For independent measurements with normally distributed instrumental error, the normalized observations should theoretically correspond to a standard normal distribution with the caveat that the filter is converged and is tuned appropriately. So the noise seen in figure 1, with level exceeding 2 or 3 represent profoundly corrupt measurements and they are weighted correspondingly less in the receiver solution.

We do not see pseudo-range noise at the same time as the range rate noise as shown in the figure 1 example. For some events, the state is sufficiently perturbed to cause errors to appear in the pseudo-range residuals. Certainly, the receiver state's velocity is corrupted when the noise appears in multiple channels.

In our evaluation of the MAGR/S we have documented other anomalies contributing to noisy ranges related to GPS receiver operation and firmware anomalies. Sources of noisy GPS velocity include:

- Sub-optimal intermediate satellite geometry due to "one at a time" changes in selected satellites. Changes have been delayed by software anomalies or poor visibility with respect to antenna gain pattern.
- Sub-optimal satellite geometry and less than 4 satellite tracking caused by signal obscuration while docked to Mir, International Space Station or Hubble Space Telescope.
- Occasional receiver restarts due to internally detected software anomalies.
- Switches of satellites tracked for navigation measurements. This is due to the Kalman filter implementation.

Noisy GPS velocity that results from the above has a different signature and often a higher magnitude than that caused by ionospheric scintillation seen in Figure 1. Furthermore, times of sub-optimal geometry and receiver resets are known and can be compared against noisy velocity periods. Space Shuttle flights of the MAGR/S, beginning in September 1996, have led to numerous receiver firmware changes. As firmware corrections were applied, the number of non-scintillation noisy velocity incidents decreased.

Scanner Code

Our approach to the data in the present work is to identify noisy periods based on the normalized delta ranges. We have identified scintillation on numerous flights. In this work we have selected 4 flights to study in detail. Referring to the normalized units in Figure 1 as "sigma level" we have written a scanner program that selects events based on that sigma level. The characteris-

tics of the selection algorithm are:

1. Sigma level exceeds 2 for 2 seconds (2 measurement cycles) or more.
2. Must be 3 seconds after a set of satellites are switched to a new channel.
3. Receiver has good lock on the satellite (FOM = 1.)

We selected a sigma level threshold of 2 based on accumulated histograms of normalized range rate observations. These indicate that greater than 2 sigma measurements are profound outliers when compared to the background distribution. Criteria number 2, reflects awareness of a known deficiency of the system in that the receiver state does not solve for range biases. When, a set of 4 satellites are assigned to hardware channels, the existing state covariance is not adjusted to reflect increased uncertainty in a new state. As a result, anomalous sigma levels appear in the measurements. Excluding events for three seconds permits influence of the satellite set switch to be absorbed into the state. The third criteria which simply masked against the internal figure of merit (FOM) evaluation of the receiver. Selecting events with good FOM, reduces effects of poor tracking due to blockage and firmware deficiency.

The event selection list does not exhaust all alternate sources for false positive detection of scintillation. For example there is statistical clustering of noisy events in range-rate immediately before a set of satellites are switched. This may be the result of some sensitivity to weak signal associated with factors contributing satellite switching logic. The issue is still under study.

Events meeting the scanner criteria are further processed to evaluate latitude and longitude, solar hour angle, and geomagnetic field at the event position. The lines of sight to all 4 satellites are computed and satellite attitude angles between the spacecraft velocity vector, the geo-magnetic field and local horizontal are also computed.

GEOGRAPHIC DISTRIBUTION

The shuttle orbits the earth approximately every 90 minutes so the low earth orbit platform

samples all geographic longitudes in a few days. Compared to ground based observations, little variation in solar hour angle is afforded. This is because the local time at a particular latitude does not vary much during the orbit and only as a result of the orbit motion of the earth around the sun during the mission and the precession of the spacecraft orbit as a result of the earth's oblateness. Evidently satellite based observations permit a wide geographic sampling with comparatively little ability to observe local time variation (at a given latitude) in the geophysical process.

Figure 2 presents the geographic clustering for four missions. Geomagnetic dip angles at +/- 15, and 45 degrees are superimposed on the plots as well as the geomagnetic equator. In the Figure 2 a inset, we see the latitude-longitude distributions for STS 88 which was flown on December

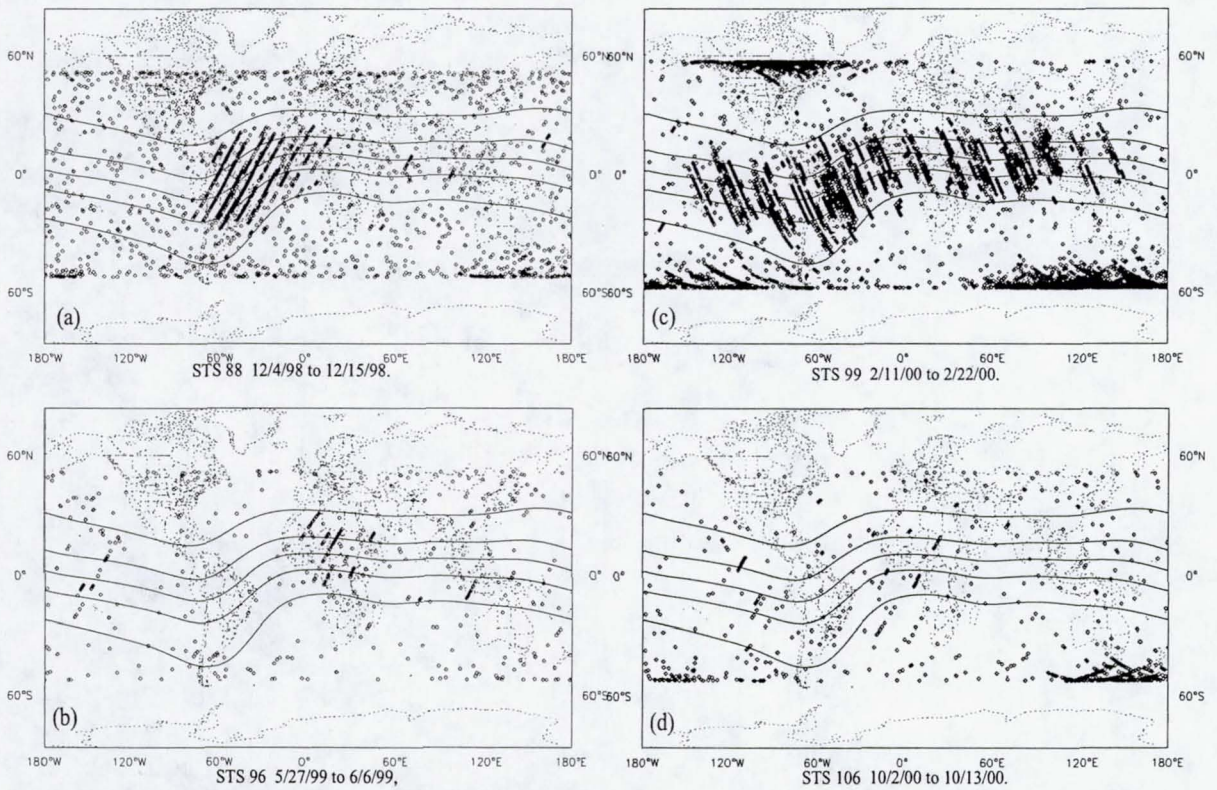

Figure 2. Geographic distribution of noise events seen in GPS receiver range rate for space shuttle. Geomagnetic equator and dip-angle contours shown at +/- 15 and 45 degrees. Wide range of activity is noted and clustering of events near the geomagnetic equator and in polar regions. The record for STS 88 seen in inset (a) may be have many false positive events resulting from now corrected firmware issues.

4 through December 15 1998. The north and south limits are dictated by the limited inclination of the orbit. There are a large number of false positive scintillation signatures in Figure 2 a which manifest as isolated events occurring through-out the plot. The significant firmware changes mentioned previously, related to errors identified during evaluation of the receiver, we believe are responsible for these false positive events. Many of the firmware issues were corrected subsequent to this flight. Nevertheless, here, in Figure 2 a we see clustering of linear trains of events along the inclined orbital tract occurring over equatorial regions of South America. These are seen on consecutive orbits, stretching eastward across the equatorial Atlantic ocean. Events taper off over the western to central sub-Saharan Africa. Other linear strings of events occur over the Indian ocean, south west of India and over Sumatra and eastward over central regions of Indonesia.

In addition, there is a hint of clustering of events near the most poleward extent of the spacecraft's orbit suggesting that we are intercepting scintillated signals through auroral zones. As a result of the large number of false positive events on STS 88 (Figure 2 a) the conclusion that we are seeing auroral scintillation is tentative. We would also caution that latitude sampling of any purely random process is biased toward higher latitudes by the approximately sinusoidal variation of latitude with respect to longitude as the spacecraft orbits. We can say that the appearance of individual time series for STS 88 that we examine for events occurring south of Australia in particular is, consistent with the morphology of scintillation signatures seen in the equatorial regions. In other words, we have confidence that we are seeing some auroral zone scintillation on STS 88 in figure 2 a.

In Figure 2 b we see the geographic distribution of scintillation events from STS 96 flown from May 27, 1999 to June 6, 1999. The results from this mission contrast to that in STS 88 seen in Figure 2 a. The number of false positive signatures is greatly reduced as a result of, we believe,

significant firmware changes mentioned previously. But in addition, the number, degree and extent of what we identify as scintillation is reduced as well. The primary contributions are from linear tracks of events along ascending portions of orbits occurring over the east-central Pacific and a group of events again occurring over central and north Africa. Indonesia appears also to be favored with a significant event during this period. It is interesting that the event over the east central Pacific ocean is isolated yet extends from the dip-angle contour at 45 degrees in the southern hemisphere all the way to the conjugate dip-latitude in the northern hemisphere. That event is accompanied by one other orbital track with greatly reduced extent.

The geographical extent of scintillation observed on STS 99 which flew from February 11 to February 22 is shown in Figure 2 c. These results are in striking contrast to those seen on STS 96 and STS 88. Here, we assert, is broad extent scintillation in the equatorial regions roughly bracketed by the dip angle contours at 45 degrees in both north and south hemispheres. The events are seen on very many consecutive orbits stretching from the east central Pacific, across South America continuing uninterrupted across the equatorial Atlantic, with some lessening of incidence across Africa but continuing over the Indian Ocean, India, South East Asia and the Western Pacific. Events are absent from the central pacific region. There is also clear evidence of polar events distributed geographically somewhat consistent with known locations of the auroral zones-polar oval systems for the geographic coverage afforded by the spacecraft orbit. These are, over east central Canada and the north central United States[7]. There is an absence of events with similar character over other northern hemisphere polar regions. In the southern hemisphere, the polar events are distributed with greatest density south of Australia and the Indian ocean. Significant activity is also present over the extreme south central Pacific. It is significant, that the equatorial zone very nearly merges with the polar events south of continental South America.

Finally, Figure 2 d presents latitude/longitude distribution of scintillation events on STS 106 which flew from October 2, 2000 to October 13, 2000. Here, scintillation is very much reduced from STS 99. Equatorial events on STS 106 are seen in the eastern Pacific and once again over Africa. Southern polar events are very much in evidence but with no apparent significant activity in the northern hemisphere for this time.

The observations are consistent with previously identified regions where scintillation is believed to occur and the seasonal variation is consistent with those published previously[3] although the STS 99 case in figure 2 c exhibits considerably broader longitudinal extent of the disturbances than the literature leads us to understand.

Instabilities

As we mentioned in our introduction, two geographic regions are of interest in contributing to disturbances in ionospheric plasma. The more important of these is the equatorial regions within about 20 to 30 degrees latitude of the geomagnetic dip equator roughly corresponding to dip angles of +/- 45 degrees. According to Anderson[8], the dynamics of the equatorial zone is controlled by a frame effect electric field which appears in response to the ionosphere being dragged across the geomagnetic field lines as a result of neutral atmosphere winds.

Since the ionospheric plasma is magnetized as a result of the earth's field, the charged electrons and ions are constrained to move in quasi circular orbits around field lines when collisions are infrequent but are relatively unconstrained in the direction parallel to the magnetic field. The field is not dipolar but can be accurately modeled as we have shown in figure 2. In equatorial regions, the field is horizontal and assumes crescent shaped arcs that are more or less meridionally oriented. As we approach a pole along a field line, the field assumes a vertical aspect or dip angle. In figure 2, we illustrate dip angle contours from a standard model corresponding to the magnetic equator,

+/- 15 and +/- 45 degrees dip angle. The 45 degree dip angle provides a logical division between equatorial and high latitudes.

As a result of the electron and ion motion being restrained across magnetic field lines, but unconstrained parallel to them, the lines tend to be equipotential and support electric fields. At low altitudes in the ionosphere, ion-neutral collision frequency is higher and currents can flow perpendicular to the field lines. The currents themselves further contribute to magnetic fields and their divergence leads to charge separation giving rise to polarization electric fields. The condition of the equatorial ionosphere is thus a complex system with competing dynamic processes involving variable and anisotropic conductivity. This, in turn, is a function of neutral atmosphere abundance and dynamics. Ultraviolet flux on the dayside and convection on the nightside contribute to ion and electron source terms while neutral atmosphere abundance and constitution provide the loss terms.

For many years, an important instability known as equatorial spread F has been known to exist. Formally spread F refers to ionogram signatures which are dispersed over frequency. These kind of observations, which have been undertaken for more than 50 years, have lead to extensive study of the ionosphere in equatorial regions. The studies identify enhanced ionospheric density know as the Appleton anomaly located at 15 to 25 degrees latitude symmetrically distributed about the magnetic equator.

It is generally believed that equatorial spread F is a result of an magnetic field-gravitational Rayleigh-Taylor mode instability in analogy to that which occurs when a layer of buoyant fluid rises though a heavier fluid. It appears that on the night side, just after dusk, production of ions from ultraviolet sunlight are shut off and chemical recombination at low altitudes rapidly erodes the ionosphere creating sharp vertical ion density gradients. This condition is maintained by the overlying horizontal magnetic field since ion motion is restrained across field lines. It is neverthe-

less energetically unstable to collapse.

The instability grows because the "falling" plasma creates horizontal currents that exhibit divergences along the gradient boundary leading to charge distributions that further feed perturbing electric fields parallel to the boundary. These then contribute to $E \times B$ drift of plasma on the boundary that further increases the amplitude of the boundary perturbation. The evolution of this instability proceeds into a non-linear magneto hydrodynamic regime which, in the theoretical models, results in upwelling of voids in the plasma that extend to altitudes of order 500 kilometers. Kelley[4] and Aarons[3] highlight the essential physics and observations that we review here including the description of plumes of ionospheric density depletions seen in backscatter radar that rise as high as 1000 kilometers.

We would also like to point out that, although we have broadly categorized equatorial events as occurring within +/- 45 degrees dip angle of the geomagnetic equator, the equatorial events extend beyond this limit in the south central Atlantic Ocean. These events are seen in figure 2 insets a, c and d. We think this is related to significantly weaker magnetic field at this location and is coincident with the well known South Atlantic Anomaly. We postulate that the crescent shaped meridionally oriented structures thought to comprise the events rise to higher altitudes and extend to wider latitudinal extent as a result of the weaker geomagnetic field which would permit greater cross field motion of ions at these points.

Furthermore, radiation hazard cited for astronaut safety in the South Atlantic Anomaly is entirely independent from processes associated with scintillation and we have no theoretical basis to assume that the high energy particles entering the earth's ionosphere in the region during geomagnetic storms are directly effective in causing scintillation of the GPS L band signals. However, coincidental thermospheric heating and changes in neutral atmosphere circulation might, we spec-

ulate, introduce variability to the process that contributes to spread F.

Scintillation is also observed in the polar regions. Much of the same complexity attached to equatorial regions also apply to the polar ionosphere. In addition, geomagnetic field lines in the high latitude regions map to the magnetosphere and the interplanetary medium connecting with the solar wind and embedded magnetic field. As a result of the non-axially symmetric contributions to the earths field and partly as a result of the attendant diurnal and space weather forcing, polar scintillation should not distribute symmetrically around the poles.

Apparently, there are two agents contributing to ionospheric disturbances at the poles. First, solar wind driven electric fields are created in the magnetosphere that map along the field lines to the polar ionosphere where sufficient collisions occur to permit limited electric field directed currents to flow. Second, during periods of geomagnetic disturbance, energetic particles enter the earths ionosphere along magnetic field lines essentially connecting to interplanetary space and interacting with the neutral atmosphere. These cause ion production and heating contributing to convection and ion density variability. Presumably, these density enhancements or depletions produce the similar effects on GPS satellite signals as the better known scintillation near the equator.

Variability from mission to mission is striking and might be explained by known seasonal and solar weather dependence of the factors that contribute to scintillation. We submit, though, that the noise we are observing is much more globally extensive and includes significant features at polar latitudes which have not been presented in the literature. As Aarons[3] points out, the known selective factors that contribute to the global scale occurrence of scintillation are modulated by neutral wind and electric field changes which are not well understood and which can theoretically either enhance or inhibit the development of the irregularities.

SOLAR ANGLE

The satellite based technique does not permit exhaustive sampling of local time as was mentioned previously. Nevertheless, we can investigate local time occurrence for the few hours local time represented by each of the flights studied. Figure 3 shows the local time occurrence divided between equatorial and polar events. Polar events are separated from equatorial events by sorting according to magnetic dip angle and forming histograms by of number of events that occurred in solar hour angle bins. From figure 2, for example, it is evident that polar events may be separated from equatorial events by the dip angle equal to 45 degrees. The only exception are those events occurring in the South Atlantic which we mentioned previously and the false positive events that are most prominent on STS 88 in figure 2 b. Figure 3, showing our solar hour distributions should not be interpreted as describing any significant composite diurnal variability. The differences in event occurrence seen between missions is certainly dominated by seasonal and space weather effects rather than a manifestation of diurnal variability.

The geophysical processes controlling equatorial spread F phenomena are associated with plasma instabilities occurring after dusk. In Figure 3 a, we show solar hour angle distributions of equatorial scintillation event. The solar hour angle trace for STS 99 shows the largest

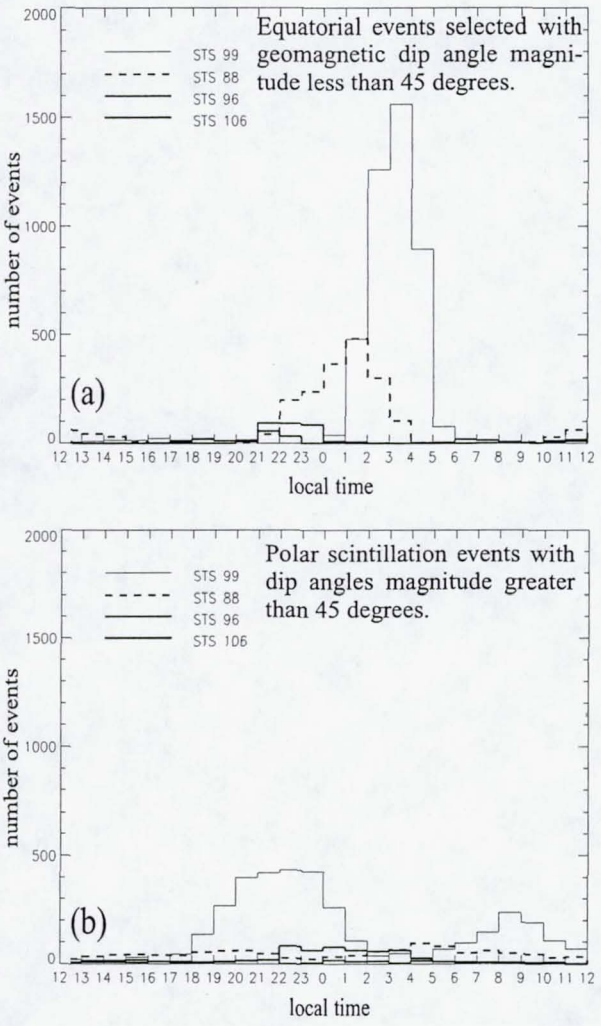

Figure 3. Solar hour angle distributions of scintillation events divided between polar and equatorial regimes. Equatorial scintillation is a nightside phenomenon.

number of events occurring primarily between 01:00 and 06:00 but we emphasize that this was the only opportunity to observe during night side passes. A comparable period of time was available on the dayside between about 12:00 and 18:00 hours for STS 99 but, as we see no significant activity evident during the period. This shows that the equatorial process contributing to the scintillation may be prominent during the time between midnight and dawn and not just during the post sunset period, a point which has also been made in the literature[9].

Similarly, the results for STS 88 show prominent equatorial activity between the hours of 22:00 and 04:00 which was the interval of time on the nightside available for observation while the opposite side of these orbits on the dayside show small elevation in activity which we can attribute to the false positive phenomenon described earlier. The events for STS 96 and STS 106 also cluster in the nightside period.

The overall impression from figure 3 a is that the equatorial scintillation we are observing is a nightside phenomenon. This is particularly established by the results from STS 99 and STS 88 where the majority of equatorial events are registered on the nightside despite equal opportunity to observe on the conjugate dayside hour angles. We would add that sampling of orbits on the nightside also explains the prominence of either ascending or descending orbit tracks seen in figure 2. For example, on STS 99 seen in figure 2 c, the predominance of descending tracks from north-west to south-east in the equatorial zone is a result of scintillation selecting those portions of the orbit on the nightside. Few ascending tracks were available on the night side.

The polar events do not have any particular diurnal clustering. The plot in figure 3 b is dominated again, by events sampled during STS 99 which is seen in the geographic latitude-longitude distribution of figure 2 c to be extensive and un-ambiguously clustered at the poleward extremes of the orbit.

INTERFERENCE PATTERN

Scintillation is thought to result from variability in both the permittivity of the ionosphere and variations in thickness of ionospheric layers between transmitter and receiver. Electrodynamic theory holds that transmitted photons exhibit interference from multiple available paths. The received signal is contributed by the paths that exhibit least first order variation in phase from one another[10]. Conventional analytical and experimental results of optics are explained using this theory. Landau and Lifshshitz draw these conclusions from their "eikonal equation" in their discussion about geometrical optics[11]. The least time principle attributed to Fermat and straight line propagation of light are derived from it.

In the ionosphere, as a result of the stochastic distribution of dispersive layers and in-homogeneities, the multiple paths over which the first order variation in phase is minimum are contributed by paths that are geometrically far apart and changing rapidly either as a result of their secular motion or as a result of the motion of the receiver. This interpretation may be at variance to a conventional view that scintillation is somehow a mixture of "phase" or "amplitude" variability and that the signal is attenuated while following a single ray to the receiver.

We view the physics of electromagnetic ionospheric propagation as the same for both of these "types" of scintillation. The distinction between phase and amplitude fading, must be related to individual variability in how receivers process range data. It has certainly been noticed that the degree of susceptibility to interference is highly receiver dependent[12]. It appears that the Shuttle's MAGR/S, employing an automatic gain control circuit, is sensitive to weak signals and thus we do not observe any conventional fading. Our receiver is quite sensitive to phase noise, explaining the observations we see in Figure 1.

Electrodynamics of Plasma

The primary contribution to index of refraction in the ionosphere may be derived from plasma theory. At the GPS L band frequencies a high frequency, cold plasma limit applies and the only contribution to permittivity is:

$$\varepsilon(\vec{x}, t) = \left(1 - \left(\frac{\omega_P(\vec{x}, t)}{\omega}\right)^2\right)\varepsilon_0 \tag{1}$$

The plasma frequency, $\omega_P(\vec{x}, t)$, which appears in equation 1, represents a normal mode frequency associated with displacement of the electrons relative to the heavy positive charge carriers in the plasma (primarily O^+ in low earth orbit.) To derive this expression, the Maxwell equations and the equation of motion for the charged species are expressed in a fourier spacial wave number, time frequency domain. Algebraic manipulation then permits a dispersion relation to be expressed which provides the analytical tool needed to understand how wavelength is related to the frequency and index of refraction in the media.

Equation 1 is a high frequency limit to that general dispersion relationship which is appropriate because all the physical cutoffs and resonance such as electron, ion gyro frequencies, plasma and hybrid frequencies are orders of magnitude smaller than the GPS signal frequency. The relative simplicity of equation 1 reflects an advantage of high frequency for use in GPS. Readers are referred to a book by Swanson[13] which we think is a good treatment on the details of this analysis. An alternate approach is the Hartree-Foch equation exposed by Klobuchar[14] which is a a formulation that explicitly and appropriately neglects motion of ions but otherwise is identical. We would like to note especially that equation 1 contains no collision or conductivity term and is positive real valued. The frequency is high enough that the mode exhibits no loss. Without a collision term there is no theoretical basis to expect a decaying amplitude as there would be in a high loss medium like sea water for example.

As the GPS signal transits the medium, the net effect is an accumulated phase shift over all pos-

sible paths between the transmitter and the receiver. For any geometric path between transmitter and receiver, the phase contribution to the total signal is computed according to:

$$\delta\phi_{S_n} = \frac{\omega}{c\sqrt{\varepsilon_0}} \int_{S_n} \sqrt{\varepsilon(\hat{x}, t)}\, dS \tag{2}$$

Equation 2 expresses the combined phase change along any arbitrary path which might even be tortuous and convoluted. The wave number is a function of the material property that is variable along the path.

Variational methods of calculus of might be used to determine a dominant path for mathematically tractible problems, but the physical principle is that all paths providing first order invariant phase to the received signal will actually contribute to the received signal. All other paths will destructively interfere and cancel out. Both the electric and magnetic fields of the wave are modulated by the interference. Conventional receivers respond to currents induced in the antenna by the electric field. So the Fourier resolution of the radiation electric field becomes:

$$\begin{aligned} E(x, t) &= E_0 \sum_n e^{i(\delta\phi_{S_n} - \omega t)} \\ &= E_0 e^{-i\omega t} \sum_n e^{i\delta\phi_{S_n}} \\ &= E_0 e^{-i\omega t}\, \Phi(\hat{x}, t) \end{aligned} \tag{3}$$

where $E_0 e^{-i\omega t}$ is the electric field at the transmitter. The summation is really taken over all available paths. The term $\Phi(\hat{x}, t)$ is a complex valued phase envelope that modulates the received signal and is a function of time and position.

Velocity Augmentation

We believe that the spacecraft velocity, being roughly 10 times greater than velocities encountered in terrestrial applications contributes to the scintillation effect. To study this, we linearize $\Phi(\hat{x}, t)$ with respect to its spacial gradients and extract information about how velocity contributes to modulating $E(x, t)$. If the vehicle's velocity is large compared to the secular motions of the geophysical processes then we propose that essentially all the noise is a result of the motion of the

spacecraft. We believe that to be the case because spread F and auroral structures in the ionosphere are persistent for several 10's of minutes whereas a low earth orbit vehicle will transit these structures in a few seconds. So, consider a velocity dependence resulting from the spacecraft velocity and spatial gradients in the envelope:

$$\Phi(\vec{x}, t) \approx \Phi(\vec{x}) + \int_0^t \vec{\nabla}\Phi(\vec{x}) \bullet \vec{V}\, dt \tag{4}$$

We would like to identify the velocity perturbation with components parallel and perpendicular to the line of sight to the scintillated satellite. The dot product in the integral in equation 4 is then expressed:

$$\begin{aligned} \frac{d\Phi}{dt} &\approx \vec{\nabla}\Phi(\vec{x}) \bullet \vec{V} \\ &= \nabla_{\|}\Phi(\vec{x})V_{\|} + \nabla_{\perp}\Phi(\vec{x})V_{\perp} \\ &= \nabla_{\|}\Phi(\vec{x})V\cos\alpha + \nabla_{\perp}\Phi(\vec{x})V\sin\alpha \end{aligned} \tag{5}$$

We argue that satellite directed components of the gradient are negligible since the accumulation of paths that are contributing to the first order variation are, in that case, nearly parallel to the line of sight. Certainly, parallel components of velocity contribute to doppler shift but the receiver is already adapted to measure this for the range rate observation. Neglecting the parallel component and substitution into equation 3 allows us to see how variations in the radiation electric field are modulated by the velocity and the phase envelope.

$$\delta E(x, t) = E_0 e^{-i\omega t} \int_0^t \nabla_{\perp}\Phi(\vec{x})V\sin\alpha\, dt \tag{6}$$

Equation 6 suggests that we test the theory by examining distributions of scintillated signal relative to the angle the line of sight makes with the spacecraft velocity vector which we here identify as α with $\alpha = 0$ denoting forward direction.

Speculation about Faraday Rotation

Since the ionospheric plasma is magnetized, Faraday rotation, a preferred phase advance of

right hand circularly polarized component of the electric field in a magnetized plasma, is a candidate for contributing to L band scintillation. Klobuchar reports that the circular polarization of GPS signals protects against Faraday rotation.[5] On the contrary, there is no physical basis for circular polarization of the GPS signal to protect against Faraday rotation as it still represents a phase advance of the electric field. Rather, the high frequency of the L band compared to any conceivable cyclotron frequencies in the ionosphere protects against first order effects from Faraday rotation. Contributions to range rate noise from rapid modulation of a Faraday rotated electric field vector resulting in scintillation is not ruled out. This might manifest as enhanced noise for lines of sight parallel to the local magnetic field.

VELOCITY ANGLE DISTRIBUTION

Identifying a null hypothesis that the signals are randomly distributed with respect to spacecraft velocity, the distribution of events with respect to angle from the velocity vector must then be proportional to $\sin(\alpha)$ because the solid angle available to intercept random lines of sight scales according to this factor. On the other hand, if signal events are proportional to the perpendicular component of velocity in accord our theory then distribution must be further scaled by another factor of $\sin(\alpha)$ since $V\sin(\alpha)$ is the component of velocity perpendicular to the line of sight as seen in equation 6.

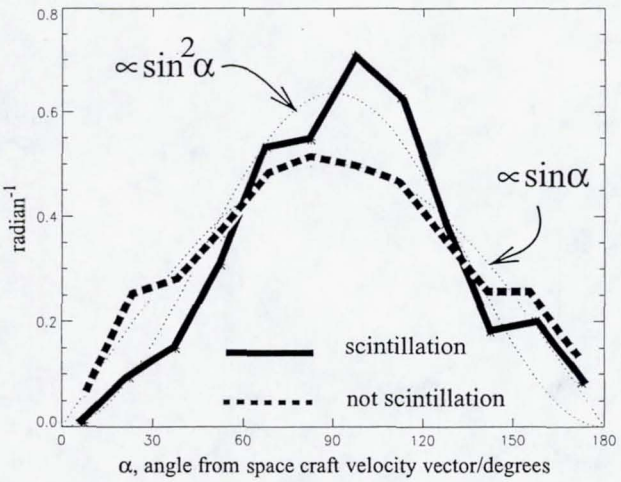

Figure 4. STS 99 data. Distribution of line of sight to GPS satellite vectors and local spacecraft velocity vector. Not-scintillated events should scale according to $\sin(\alpha)$ whereas the scintillated signals should distribute according to $\sin^2(\alpha)$. All series shown are normalized to unit integral with respect to α.

To test this, we accumulate statistics on the line of sight of scintillation events ($\sigma >$

2) compared to contemporaneous un-scintillated measurements ($\sigma < 2$). These data were prepared by calculating the angle between the GPS satellite line of sight and the spacecraft velocity vector. Nominally, 4 satellites are tracked simultaneously. Distributions of angles are divided into two sets based on noise level. On STS 99 for example, we found 10308 scintillation events characterized by noisy delta range ($\sigma > 2$). In this set we also found 25266 satellite tracking intervals which exhibiting just nominal signal level. Figure 4 presents the results. These histograms are normalized to unit integral with respect to angle. Normalized distributions of $\sin(\alpha)$ and $\sin^2(\alpha)$ are presented for reference.

We assert that scintillated events follow a $\sin^2(\alpha)$ distribution consistent with our theory while the "random" line of sights conform closely to the $\sin(\alpha)$. Although we have not ruled out other possible selective factors such as latency in acquiring lock on satellites in the forward direction for example. The same analysis for STS 88 supports the theory. The same analysis for the two other missions studied have less statistical confidence but do not contradict it.

We are aware that the satellite selection algorithm for the GPS receiver is not strictly random. The receiver attempts to track 4 satellites with an optimal geometry. This puts an emphasis on selection of one high elevation satellite and 3 other low elevation satellites. We are not able to rule out an accidental clustering of scintillation according to a $\sin^2(\alpha)$ distribution, but we would not understand how to reconcile this with the $\sin(\alpha)$ of the non-scintillated satellite tracks. We would expect that these latter events would be depleted near 90 degrees if we were accidentally selecting high elevation satellites that were also scintillated. We should also point out that the selection logic permits satellites to track over significant arcs of the sky so that a high elevation satellite eventually becomes low elevation.

MAGNETIC FIELD

Plasma instabilities contributing to the spread F anomaly are restricted in motion to co-rotating flux tubes that are oriented along geomagnetic meridians. The importance of the magnetic field to mobility of ions and our suggestion that transient Faraday rotation contributes to scintillation encourages us to consider examining event distribution with respect to the angle of the line of sight using the same kind of analysis we performed for the velocity. Figure 5 represents our effort in this regard. Here, we have accumulated a histogram of number of events in bins of angle of the line of sight from the geomagnetic field at the location of the spacecraft. As we have mentioned previously, solid angle measures of random distributions are weighed toward perpendicular as a result in the increase in available solid angle as the perpendicular direction is approached. To compensate for this in figure 5 we have weighted the histogram bins so that the width of bins are proportional to the arc-cosine of the solid angle. The histograms are also normalized to unit integral with respect to angle.

There were 3635 scintillated of 12889 total events with dip angle magnitude less than 45 degrees. STS 99 and the other missions are similar. Although there is some tendency to elevated levels at 0 and 180 they are not supported statistically and we have not ruled out other coincidental reasons for that effect. We therefore report a null result for substantial clustering of the events with respect to angle between the magnetic field and line of sight to GPS satellites. We would like provoke further discussion in this area.

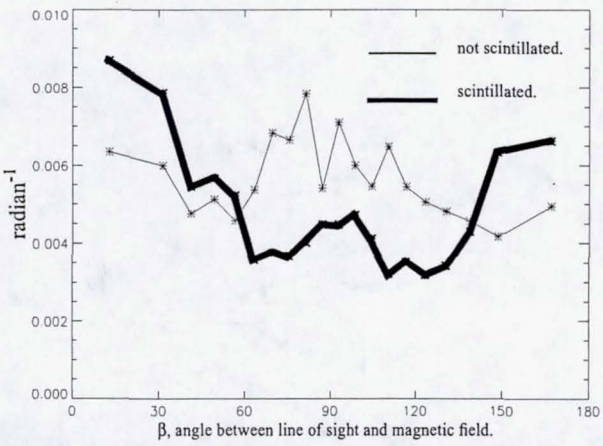

Figure 5. Distribution of angles between satellite line of sight and geomagnetic field at location of spacecraft for the equatorial scintillation events from STS 88. Histogram bins are scaled according to equally spaced increments of $\cos^{-1}(\beta)$ compensating for $\sin(\beta)$ distribution of solid angle.

CONCLUSION

The essential physics of radiation through the ionosphere predicts that the medium will not attenuate at L band frequencies. Scintillation occurs because there exists multiple available paths of propagation that are geometrically far apart and rapidly varying. Thus, amplitude fading and phase scintillation are not distinct physical phenomenon but rather reflect individual idiosyncratic receiver responses to the same interference envelope.

The GPS receiver selected for use on the Space Shuttle is subject to a spacecraft velocity augmented modulation of the interference envelope affecting range rate observables. The interference occurs in the geographic regions and at solar hour angles consistent with previously identified ionospheric instabilities that cause scintillation.

The incidence of observed scintillation is highly variable. Equatorial events occur at night and cluster to within 20 to 30 geographic degrees of the magnetic equator corresponding to a dip angle boundary between + or - 45 degrees except for a few excursions outside that zone in the south central equatorial Atlantic Ocean. The equatorial zone that we identify coincides with the location of ionospheric plasma instabilities identified with equatorial spread F. Local time occurrence is consistent with that conclusion although we see it occurring at later hours in the night than the most of the literature. Polar events correspond to the auroral regions and exhibit known asymmetries consistent with the polar auroral oval systems.

The scintillation we observe in the MAGR/S is apparently augmented by high velocity of the spacecraft because events are preferentially distributed at right angles to spacecraft motion in accord with a theory we advance holding that the component of spacecraft motion perpendicular to the line of sight contributes to the interference. This appears to be the case at least for the MAGR/S receiver we are studying. If these observation are repeatable and the theory further substantiated we would like offer it as a selective factor in weighting measurements for future space

rated receivers. The angle between the velocity vector, and the line of sight to the GPS could be used to increase the formal measurement uncertainty of measurements when the angle is close to perpendicular. We propose that this can mitigate high error in associated velocities.

The widespread geographical distribution and apparent seasonal variability is striking and much greater than we are led to understand based on the current body of literature. We submit that the known selective factors such as magnetic activity are modified, even as Aarons[3] points out, by seasonal or synoptic scale variability in the neutral atmosphere abundance and neutral winds as these are the parameters least well understood.

ACKNOWLEDGMENTS

These materials are sponsored by the National Aeronautics and Space Administration under Contract NAS9-20000.

REFERENCES

1 Goodman, J. L. and Kramer, L., "Scintillation Effects On Space Shuttle GPS Data," *Proceedings of the National Technical Meeting*, Institute of Navigation, Long Beach, CA, January 22-24, 2001.

2 Goodman, J.L., "Parallel Processing GPS Augments TACAN in the Space Shuttle," GPS World, Vol. 15, No. 10, October 2002, pp. 20-26.

3 Aarons, J., "The Longitudinal Morphology of Equatorial F-layer Irregularities Relevant to their Occurrence," *Space Science Reviews*, Vol. 63, 1993, pp. 209-243.

4 Kelley, M. C., "The Earth's Ionosphere: Plasma Physics and Electrodynamics," Academic Press, Inc., 1989.

5 Klobuchar, J.A., "Ionospheric Effects on GPS," *Global Positioning System: Theory and Applications,* edited by Parkinson, B.W, Spilker Jr., J.J. et al. AIAA, 1996, pp. 485-515.

6 Pi, X, A.J. Mannucci, U.J. Lindqwister, Ho., C.M., "Monitoring of Global Ionospheric Irregularities Using the Worldwide GPS Network," *Geophysical. Research. Lettters.*, Vol. 24, No. 18, 1997, pp. 2283-2286.

7 Bishop, G., Basu, S., Holland, E., Secan, J., "Impacts of Ionospheric Fading on GPS Navigation Integrity," *Proceedings of ION GPS-94*, 1994, pp. 577-585.

8 Anderson, D. N., "A Theoretical Study of the Ionospheric F Region Equatorial Anomaly-II. Results in the American and Asian Sectors," *Planetary and Space Science*, Vol. 21, 1973, pp. 421-442.

9 Whalen, J.A. "Equatorial Bubbles Observed at the North and South Anomaly Crests: Dependence on Season, Local Time and Dip Latitude," *Radio Science*, Vol. 32, No. 4, 1997, pp. 1559-1566.

10 Feynman, R. P., "QED: The Strange Theory of Light and Matter," Princeton University Press, Princeton, New Jersey, 1985.

11 Landau, L. D., and Lifshitz, E. M., "The Classical Theory of Fields," Pergamon Press, Oxford, 1975.

12 Doherty, P. H., Delay, S. H., Valledares, C. E., Klobuchar, J. A., "Ionospheric Scintillation Effects in the Equatorial and Auroral Regions," *Proceedings of ION GPS-2000*, 2000, pp. 662-671.

13 Swanson, D.G., "Plasma Waves," Academic Press, 1989.

14 Klobuchar, J.A., "Real-time Ionospheric Science: The New Reality," *Radio Science*, Vol. 32, No. 5, 1997, 1943-1952.